Evidence of Microscopic-Scale Modifications in Optical Glasses Supporting Second Harmonic Generation

C. Cabrillo, G.J. Cuello. P. García-Fernández and F.J. Bermejo
Instituto de Estructura de la Materia, Serrano 123, Madrid E-28006, Spain

V. Pruneri, F. Samoggia and P. G. Kazansky
Optoelectronics Research Centre, University of Southampton, Southampton S017 IBJ, United Kingdom

S.M. Bennington
Rutherford Appleton Laboratory, Chilton, Didcot, Oxon, OX11 0QX, United Kingdom

(October 7, 1998)

We explore the extent of changes in dynamic correlations of vitreous SiO_2 induced by treatments required to enable frequency doubling of infrared light (poling) by means of inelastic neutron scattering. These appear as an excess of modes in certain regions of the frequency spectrum as well as a narrowing of the 100 meV peak. Such alterations are better ascribed to a change in ordering of the material than to the emergence of "defect" modes, absent in the native sample.

42.70, 63.70.+x, 78.20.-e, 42.65.Ky

The ability of optical fibers to generate visible (green) light via Second Harmonic Generation (SHG) after strong irradiation by infrared laser light, first detected in 1985 [1] surprised the optical community since a fundamental principle for the second-order optical susceptibility tensor [2], forbids SHG (i.e. optical frequency doubling) in an isotropic material, such as amorphous silica. Moreover, a well defined phase matching between the interacting waves is required to allow constructive interference leading to efficient SHG. As a matter of fact, even if ways leading to the emergence of some symmetry-breaking mechanism could be be thought-off, the phase matching condition seemed far more difficult to fulfill.

A number of meso- or macroscopic modifications within the glassy matrix are known to be associated with laser poling. Such alterations, as judged by the ability of the material to sustain SHG, are long lasting (on the scale of months) and changes in the macroscopic mechanical properties of glass fibers (large increase in brittleness) resulting from laser treatments have been reported [7].

A plausible explanation for the origin of the phenomenon was put forward by Dianov *et al.* [3]. There, the emergence of a spatially modulated local dc field, E_0, which, via a third-order nonlinearity ($\chi^{(3)}$) which is finite in isotropic materials, induces a spatially modulated second order nonlinearity ($\chi^{(2)} \propto \chi^{(3)} E_0$) able to double the pump frequency. This mechanism, known as Electric Field Induced Second Harmonic Generation (EFISHG), postulates that a dc field is induced by photocurrents originated from ionization of color centers associated with impurities in the glass structure. In the simplest model [3], quantum interference between two and one photon ionization leads to a spatial modulation of the current, resulting in a phase matching (or more aptly, quasi-phase matching). This happens as a consequence of a frozen-in dc field which is generated once the electric charges set in motion by the photocurrents are pinned down by "defects". Under such conditions, inversion symmetry breaks down under the local dc field without concomitant changes in structure.

A substantial effort has since then been focused towards the achievement of a permanent $\chi^{(2)}$ and to improve the SHG efficiency in optical glasses. Alternative techniques to poling by means of intense laser irradiation have been found. In particular the one referred to as "thermal poling", consisting in the application of a high voltage ($\sim$ 5 kV, just below dielectric breakdown of the material) to thin glass plates at rather moderate temperatures ($\sim 270°C - 300°C$, compared with $\approx$ 1200°C where the glass melts to a supercooled liquid) is able to provide figures for SHG conversion comparable to those shown by anisotropic materials (inorganic crystals [4]). There is a dearth of studies on the microscopic structure and/or dynamical alterations associated with poling. Most results are macro- [5] or mesoscopic [6] in nature. Up to now, probably the most direct investigation of the phenomenon comes from Raman spectroscopy [7,8]. Significant changes between poled and native fibers were observed at rather well defined frequencies and interpreted as changes in the density of some topological "defects" within the glass, which were assumed to lead to symmetry-breaking thus enabling SHG [9]. A direct interpretation of the Raman data is, however, hampered by the need of previous knowledge of the possible structural alterations in order to properly assess the concomitant variations in the Raman matrix elements governing the signal intensities. Our aim here is to investigate the microscopic mechanisms leading to the appearance of the

SHG response in poled glasses, using neutrons as a probe which directly couples to the nuclei. Even if the technique is severely limited by intensity, it is expected that the very strong treatment applied to the glassy material, will result in measurable differences between native and poled glasses. The choosing of "thermally poled" samples was motivated by the fact that this seems the most promising process applicationswise. We thus carried out a set of inelastic neutron scattering (INS) measurements covering the frequency range where previous reports from optical spectroscopies found differences between native and poled samples.

The samples were made of electrically-fused quartz (Infrasil from Heraeus) with dimensions 40 × 40 × 0.1 mm. The thickness ($\sim 100\mu$m) was chosen as the smallest possible in order to increase the poled/unpoled volume ratio. In fact, after treatment [4], the nonlinearity is confined to a region $\sim 5\mu$m deep under the anode surface regardless of the sample thickness, so that the convenience of using thin samples is evident. A ratio of poled/unpoled material of $\sim 5\%$ was estimated. Poling was carried out at 275°C with an applied dc voltage of ~ 5 kV for 40 minutes. The poled sample consisted in fifteen plates stacked together. For comparison a similar stack of unpoled samples was used.

The measurements were performed using the MARI spectrometer at the ISIS pulsed neutron source at the Rutherford Appleton Laboratory, Oxfordshire (UK). Two different incident energies were used (220 meV and 150 meV) which enabled covering kinematic ranges with different resolution in energy-transfers. The samples were kept at 20 K in order to reduce the multiple-phonon contribution to the spectrum, a quantity which becomes substantial in measurements of this kind performed at room temperature. For a macroscopically isotropic material such as a glass, the quantity of utmost importance to specify the dynamics is the $Z(\omega)$ spectral frequency distribution (or vibrational density of states), since there is no such a thing as a Bloch vector in terms of which dispersion relations may be defined. For samples where the dominant neutron-nucleus scattering is of incoherent nature, derivation of $Z(\omega)$ from the measured double differential cross-section only involves a few corrections. In the case of silica, where scattering from Si and O nuclei gives rise to coherent (interference) effects, the derivation of $Z(\omega)$ from the measured data becomes more elaborated. A number of schemes for averaging-out the coherent effects have been developed and are known to lead to reliable estimates of the spectrum, as attested by comparison of the low-temperature specific heat evaluated from $Z(\omega)$ on quasi-harmonic grounds against experimental thermal data. In our particular case we have adopted a procedure described in detail in Ref. [10] which is based on a phonon expansion of the dynamic structure factor $S(Q,\omega) \propto \mathrm{d}^2\sigma/\mathrm{d}\Omega\mathrm{d}E$ and consists in an iterative scheme designed to correct a number of instrumental and sample-dependent (multiphonon) effects, and has been shown to give results in good agreement with thermodynamic data [10].

A sample of $S(\omega)$ spectra which represents an angular average over all detectors for frequencies above 30 meV is shown in Fig. 1. A schematic drawing of the polarized (HH) Raman response from vitreous silica is shown in the inset for comparison purposes. The derived density of states for the native material was then calculated from such an average. The same procedures were followed to derive the spectra for both poled ($Z_p(\omega)$) and native ($Z_u(\omega)$) materials. Any possible systematic error in estimating the frequency distribution should therefore be cancelled out in the $Z_p(\omega) - Z_u(\omega)$ difference function.

The Fig. 2 displays a comparison between the spectral distributions for native and poled samples up to a frequency of 120 meV ($\approx 960\ \mathrm{cm}^{-1}$). The spectrum for the native sample can readily be compared with estimates for the same magnitude measured under different conditions [11]. As main features it shows a low frequency region (limited by resolution effects) with a shoulder at 20 meV, a maximum at about 53 meV and a narrow peak at 100 meV. Additional structure appears at higher frequencies such is the well known double peak with maxima at 135 meV ($\approx 1080\ \mathrm{cm}^{-1}$) and 150 meV ($\approx 1200\ \mathrm{cm}^{-1}$) meV.

The assignment of the referred features to microscopic "modes" still is a matter of debate. The simpler models aimed to describe the spectrum on the basis of calculations carried out for continuous random networks of $Si(O_{1/2})_4$ tetrahedra with central forces only [12] or on Bethe lattices [13]. Under such assumptions, most of the spectrum below 20 meV is left unaccounted since it is within this range of frequencies where the effects brought by the absence of large scale regularities in the real materials become more marked. The dominant features are then assigned on the basis of band-edge frequencies [12] of an infinitely extended coordinated tetrahedral AX_2 network connected by springs. The broad peak about 53 meV would there correspond to the so called ω_1 mode where the oxygens undergo a symmetric stretch whereas the Si atoms are still. That appearing at ≈ 100 meV is assimilated with the ω_3 mode where all atoms move and the pair of higher frequency peaks are assigned as arising from LO−TO splitting, the higher frequency (150 meV) being identified with the ω_4 vibration. The model is supplemented by two "defect" modes which were introduced to explain the origin of the two narrow D_1 and D_2 Raman lines appearing at ≈ 61 meV ($495\ \mathrm{cm}^{-1}$) and ≈ 75 meV ($606\ \mathrm{cm}^{-1}$) (see inset of Fig. 1). Their origin is sometimes ascribed to the presence of intermediate-range-order which manifests itself by three and fourfold planar ring structures. Although such a model has over the years constituted a basis to rationalize the Raman spectrum, it now seems to portray a simplified view of the complicated atomic dynamics within the glass. In fact, a comparison of the experimental $Z(\omega)$ shown in

Fig. 2 with the Raman spectrum shows that the INS distribution is substantially broader (well beyond resolution effects) than the former. In particular, and central to our case, the D_1 and D_2 lines are not identifiable with clear features in the INS spectra. Instead, a broad irregular structure appears between 60 meV and 85 meV as shown in Fig. 2 (also present in previous experiments [11]).

The picture arising from computer simulations portrays the dynamics of this material as substantially more complex and, in fact, recent results on the origin of the sharp peaks in the spectrum of network glasses [14] show that the basic structural requirement for narrow peaks is the presence of ring fragments only (i.e., the planarity and regularity of those are not fundamental). In the present case however our interest is focussed on *differences* between the spectrum of the material subjected to disparate treatments and therefore, an accurate description of all the spectral features is well beyond scope.

As stated above, the frequencies explored here comprise those where Raman studies found changes induced by poling. In spectra shown in Fig. 1, a measurable difference between poled and unpoled glasses is readily seen for about 53 meV (≈ 424 cm^{-1}), a band comprising 60 meV (≈ 480 cm^{-1}) $\leq E \leq$ 95 meV (≈ 760 cm^{-1}) and the peak at 100 meV (≈ 800 cm^{-1}).

The changes persist once the spectrum is transformed into a vibrational density of states, a quantity directly comparable with Raman data shown schematically in the inset of Fig. 1. Such differences, especially on the band about 60 meV have to be regarded as rather large. In fact they are comparable in magnitude to those exhibited by densified silica, if compared with the normal density material [11]. On the other hand, as shown in the the lower frame of the graph, the differences are outside error bars and this supports the statistical significance of such findings. The measurements carried out using a larger incident energy (220 meV) confirmed the above mentioned changes and enabled the exploration of the spectral region extending up to 180 meV (≈ 1440 cm^{-1}), which comprises the strong double-peak structure referred above [15]. No significant changes upon poling were found within that range of frequencies. In consequence, the ensuing discussion will only concern alterations below 110 meV. From computer simulations using realistic potentials for the interparticle interactions [16], we know that in the frequency range, where the material response is modified by poling, the vibrational dynamics still shows substantial "collective" character, even if what is left at such high frequencies can only be considered as remnants of long-wavelength phonons which become at these scales heavily damped and hybridized with vibrations of "optical" character. Such vibrations are usually extended, that is involve the concerted motions of relatively large (20-60 [16–18]) groups of atoms. One could therefore expect that motions of this kind would be more easily affected by strong environmental effects such as the strong applied dc fields which are "frozen-in" after removal of the poling field than others involving highly localized "defects". From this perspective, no substantial changes in the pattern of short-range chemical bonding are necessarily required.

In addition, two more spectral features are clearly affected by poling, i.e., the increase in the intensity of the broad peak centered at 53 meV and the narrowing of the 100 meV peak. A recent analysis [19] shows how disorder alters the peak heights of the density of modes owing to coupling between close enough modes. Whether this gives rise to an increase or a decrease depends on the specific case. The observed enhancement of the 53 meV peak could then signal a change in ordering. Given the highly anisotropic nature of the poling process, one would expect an increase in ordering. Such a picture is strongly supported by the narrowing of the 100 meV peak. The fact that ordering should produce narrowing is not only physically plausible, but is also supported by calculations. Indeed, the results of Ref. [19] predict such an effect too. More explicitly, Bethe lattice calculations demonstrate that the main effect of a reduction on the spread of the inter-tetrahedral angle distribution is a narrowing of the 100 meV peak [20], precisely the most intuitive kind of ordering that would be expected from the poling process. It remains an open question whether such ordering is a significant contribution to the measured optical second order nonlinearity.

In summary, the alterations occurring in fused silica at a microscopic level after the material is subjected to "thermal poling" are revealed from INS. From the present data two main conclusions are drawn. First, the modifications which occur within a frequency range encompassing the so called D_1 and D_2 Raman lines are consistent with dynamical alterations involving rather large groups of atoms. This finding is in contrast with the highly localized features expected if poling would involve the emergence of "defects", a mechanism sometimes assumed as the one responsible for the second order nonlinear optical response. Secondly, alterations around 53 meV and particularly at 100 meV are suggestive of an ordering process in the treated material implying a reduced spread in the inter-tetrahedral angle distribution. Further studies are needed to clarify whether these changes can justify the value of second-order nonlinearities measured after poling.

I. ACKNOWLEDGMENTS

Work supported in part by grants No. TIC95-0563-C05-03, No. PB96-00819, CICYT, Spain, and Comunidad de Madrid 06T/039/96. V. Pruneri and F. Samoggia acknowledge Pirelli Cavi (Italy) for their fellowship and studentship respectively.

[1] U. Osterberg, W. Margulis, Opt. Lett. **11**, 516 (1986).
[2] A. Yariv, P. Yeh, *Optical waves in crystals*, Wiley, 1984, p. 504.
[3] E.M. Dianov, P.G. Kazansky, D.Yu. Stepanov, Sov. Lightwave Commun. **1**, 247 (1991).
[4] R. A. Myers, N. Mukherjee and S. R. J. Brueck, Opt. Lett. *16*, 1732 (1991).
[5] V. Mizrahi *et al.*, Opt. Lett. **13**, 279 (1988).
[6] W. Margulis, F. Laurell, B. Lesche, Nature **378**, 699 (1995); P. G. Kazansky *et al.*, Appl. Phys. Lett. **68**, 269 (1996).
[7] J.M. Gabriagues, H. Fevrier, Opt. Lett. **12**, 720 (1987);
[8] A. Kamal, D. A. Weinberger and W. H. Weber, Opt. Lett. **15**, 613 (1990);
[9] R. H. Stolen and H. W. K. Tom, Opt. Lett. **12**, 585 (1987).
[10] J. Dawidowski, F.J. Bermejo, R. Fayos, R. Fernández Perea, S.M. Bennington, A. Criado, Phys. Rev. E **53**, 5079 (1996).
[11] M. Arai *et al.*, Physica B **180** & **181**, 779 (1992).
[12] P. N. Sen and M. F. Thorpe, Phys. Rev. B **15**, 4030 (1977).
[13] M.F. Thorpe in *Excitations in disordered systems*, Plenum New York, 1982, p. 85.
[14] R. Fernández-Perea, F.J. Bermejo and M.L. Senent, Phys. Rev. B**54**, 6039 (1996).
[15] J.M. Carpenter and D.L. Price, Phys. Rev. Lett. **54**, 441 (1985); M. Arai *et al.*, Trans. Am. Cryst. Assoc. **27**, 113 (1991).
[16] S.N. Taraskin and S.R. Elliot, Europhys. Lett. **39**, 37 (1997).
[17] H.R. Schober, C. Gaunke ans C. Oligschleger, Prog. Theor. Phys.Suppl **126**, 67 (1997).
[18] R. Fernández-Perea, FJ Bermejo and E. Enciso, Phys. Rev. B**53**, 6215 (1996).
[19] M. Marinov, N. Zotov and L. Konstantinov, Z. Phys. B **101**, 219 (1996).
[20] F.L. Galeener in *Disorder in Condensed Matter Physics*, J.A. Blackman and J. Tagüeña (Eds.). Oxford Science Publications. The Clarendon Press, Oxford, 1991, p. 45.

FIG. 1. Angular averaged spectra for the range of frequencies where alterations due to poling are manifest. The inset depicts an schematic representation of the HH-polarized Raman spectrum of bulk v-silica, showing the location of the D_1 and D_2 defect modes.

FIG. 2. The $Z(\omega)$ frequency distribution of both, the native (solid line) and poled (dashed line) samples and the difference between them. Error bars in $S(\omega)$ ($\sigma_S(\omega)$) are proportional to the square root of the number of counts in each detector. For the DOS, the error bars are obtained taking the semidifference between the DOS calculated with $S(\omega)+\sigma_S(\omega)$ and $S(\omega)-\sigma_S(\omega)$ as input. After a smoothing process over five points, the error was divided by $5^{1/2}$.

Fig. 1

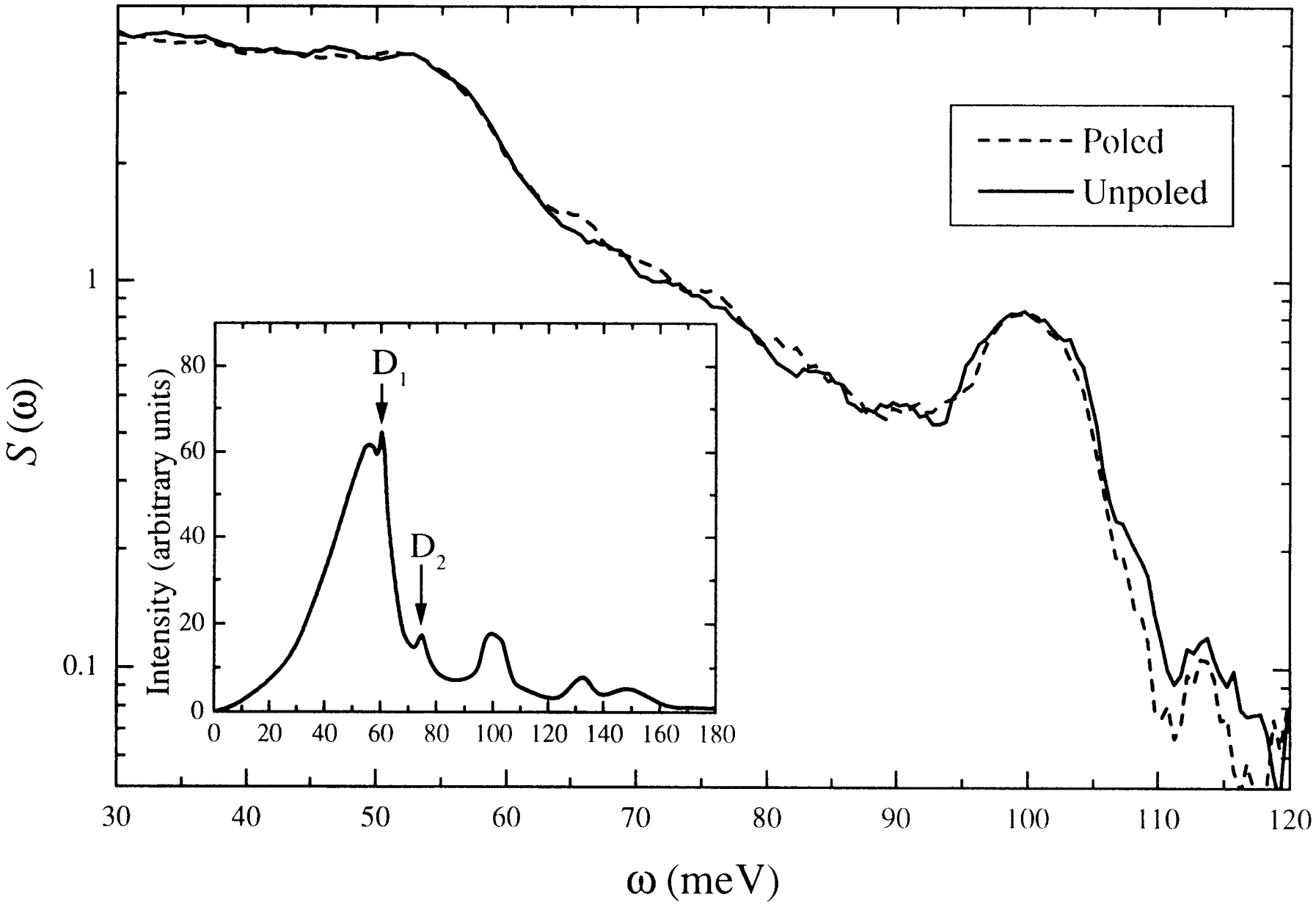
Poled
Unpoled
S (ω)
1
0.1
30
40
50
60
70
80
90
100
110
120
ω (meV)
Intensity (arbitrary units)
D1
D2
0
20
40
60
80
100
120
140
160
180

Fig. 2

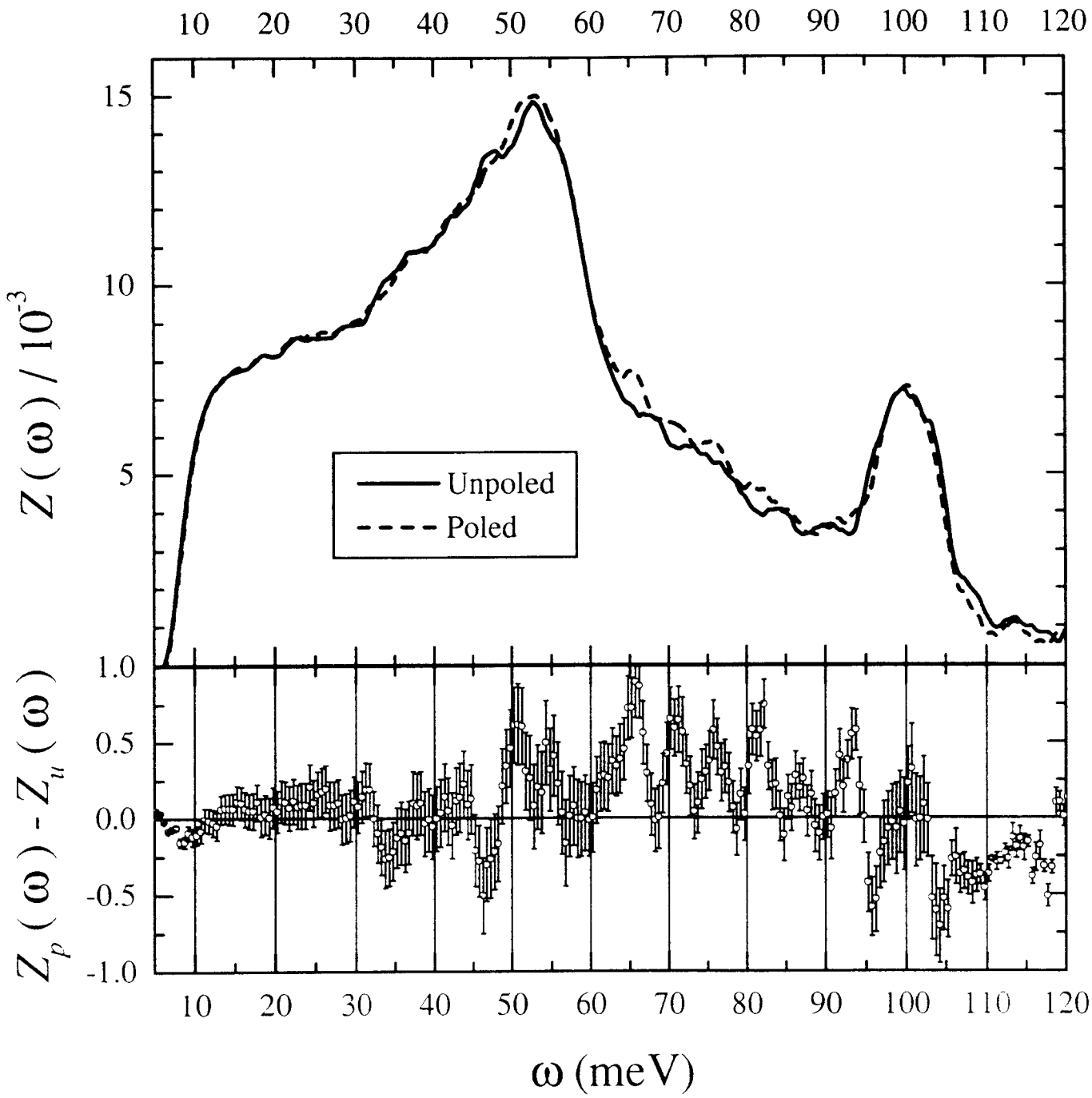
10 20 30 40 50 60 70 80 90 100 110 120
15
10
5
1.0
0.5
0.0
-0.5
-1.0
Z (ω) / 10^-3
Z_p (ω) - Z_u (ω)
Unpoled
Poled
ω (meV)